

# Suzaku X-Ray Study of an Anomalous Source XSS J12270–4859

Kei SAITOU,<sup>1,2</sup> Masahiro TSUJIMOTO,<sup>1</sup> Ken EBISAWA,<sup>1</sup> and Manabu ISHIDA<sup>1</sup>

<sup>1</sup>*Japan Aerospace Exploration Agency, Institute of Space and Astronautical Science*

*3-1-1 Yoshino-dai, Sagami-hara, Kanagawa 229-8510*

<sup>2</sup>*Department of Astronomy, Graduate School of Science, The University of Tokyo, 7-3-1 Hongo, Bunkyo-ku, Tokyo 113-0033*

*ksaitou@astro.isas.jaxa.jp*

(Received 2009 April 9; accepted 2009 April 28)

## Abstract

We report the results of the Suzaku X-ray observation of XSS J12270–4859, one of the hard X-ray sources in the INTEGRAL catalogue. The object has been classified as an intermediate polar (IP) by optical spectra and a putative X-ray period of  $\sim 860$  s. With a 30 ks exposure of Suzaku, we obtained a well-exposed spectrum in the 0.2–70 keV band. We conclude against the previous IP classification based on the lack of Fe  $K\alpha$  emission features in the spectrum and the failure to confirm the previously reported X-ray period. Instead, the X-ray light curve is filled with exotic phenomena, including repetitive flares lasting  $\sim 100$  s, occasional dips with no apparent periodicities, spectral hardening after some flares, and bimodal changes pivoting between quiet and active phases. The rapid flux changes, the dips, and the power-law spectrum point toward the interpretation that this is a low-mass X-ray binary. Some temporal characteristics are similar to those in the Rapid Burster and GRO J1744–28, making XSS J12270–4859 a very rare object.

**Key words:** stars: binaries: close — stars: individual (XSS J12270–4859) — stars: variables: other — X-rays: stars

## 1. Introduction

Intermediate polars (IPs) are a subclass of cataclysmic variables (CVs), which are interacting binaries of a moderately magnetized ( $10^5 - 10^7$  G) white dwarf (WD) with a late-type dwarf or giant companion. Accreting material from the secondary forms a disk around the WD, which is truncated by the magnetic field in the primary's vicinity. Defining features of IPs are (1) optical and X-ray modulation due to the spin and orbital motions, (2) hard X-ray emission with Fe  $K\alpha$  features arising from the accretion shock at the base of the accretion column, and (3) a complex profile of X-ray absorption (Patterson 1994; Warner 1995; Ezuka & Ishida 1999; Ramsay et al. 2008).

IPs occupy a very small fraction of CVs; about 50 confirmed IPs account only for  $\sim 2\%$  of catalogued CVs (Downes et al. 2001; Barlow et al. 2006). Nevertheless, their particular brightness in the hard X-rays to soft  $\gamma$ -rays makes IPs to stand out when the sky is seen in these bands. The INTErnational Gamma-Ray Astrophysics Laboratory (INTEGRAL) serves very well for this purpose. A total of 21 CVs, mostly IPs, are listed in the third source catalogue by the INTEGRAL Soft Gamma-Ray Imager (ISGRI; Bird et al. 2007). These include newly discovered samples, which was made possible by the ISGRI's positional accuracy of  $\lesssim 1'$  and systematic optical spectroscopic follow-up studies (Masetti et al. 2004).

XSS J12270–4859 (hereafter J12270) is one of such sources. Initially discovered in the Rossi X-ray Timing Explorer (RXTE) slew survey (Revnivtsev et al. 2004), the source was classified as an IP based on the H and He

emission lines in the optical spectra (Masetti et al. 2006). This claim is also supported by a hint of  $\sim 860$  s X-ray periodicity in the RXTE data (Butters et al. 2008).

Accumulating evidence, however, poses doubt on the IP classification. The Fe  $K\alpha$  features remain undetected and the complex absorption profile is absent in the X-rays (Butters et al. 2008; Landi et al. 2009). Optical monitoring failed to confirm the reported X-ray period, but instead found flickering and possible phase changes with different temporal behaviors (Pretorius 2009). All these features disagree with the IP nature of this source.

In this Letter, we examine the previous IP classification of J12270 based on the new X-ray data with Suzaku. We present a well-exposed spectrum and a 30 ks light curve to test the Fe  $K\alpha$  emission, and the modulation and the rapid changes in flux. We conclude against the IP classification and propose that J12270 is rather a low-mass X-ray binary (LMXB) full of anomalous temporal behaviors.

## 2. Observation and Data Reduction

We observed J12270 with Suzaku (Mitsuda et al. 2007) on 2008 August 8–9. Suzaku has two instruments: the X-ray Imaging Spectrometer (XIS; Koyama et al. 2007) at 0.2–12 keV and the Hard X-ray Detector (HXD; Takahashi et al. 2007; Kokubun et al. 2007) at 10–600 keV.

The XIS is equipped with four X-ray CCDs at the foci of four co-aligned X-ray telescopes (Serlemitsos et al. 2007). One of them (XIS 1) is back-illuminated (BI) and the others (XIS 0, 2, and 3) are front-illuminated (FI) devices, which have an energy resolution of 150–190 eV

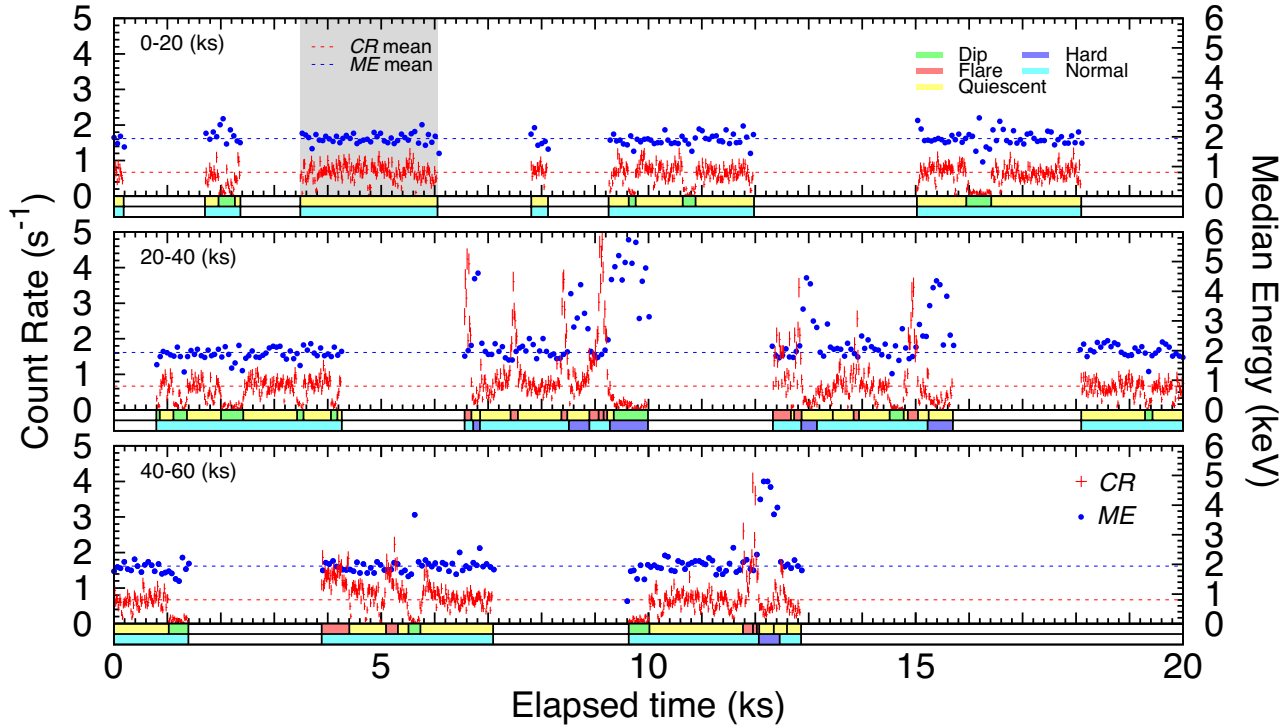


**Fig. 1.** XIS light curves of the background-subtracted  $CR$  (red crosses) and the  $ME$  (blue bullets) in 0.2–12.0 keV. The curves are folded by 20 ks. The  $CR$  and  $ME$  curves are binned respectively with 16 and 64  $s\ bin^{-1}$ . The origin of the abscissa is the observation start at 54686.97628 d in the modified Julian date. The  $1\sigma$  Poisson error is indicated for  $CR$ . The means of  $CR$  and  $ME$  determined in a quiescent interval (gray shaded region) are represented by broken lines. The two horizontal bars at the bottom of each panel represent segmented blocks with different colors for dips, flares, and quiescence for  $CR$  and hard and normal for  $ME$ .

(FWHM) at 5.9 keV. XIS 2 has been dysfunctional since 2006 November. Combined with the telescopes, the XIS has a total on-axis effective area of 1030  $cm^2$  at 1.5 keV and a field of view (FoV) of  $18' \times 18'$ . The XIS was operated using the normal clocking with a frame time of 8 s.

The HXD is a non-imaging detector comprised of several components covering different energy ranges. We focus on the PIN detector sensitive at 10–70 keV, which has an energy resolution of 3.0 keV (FWHM), a time resolution of 61  $\mu s$ , and an effective area of  $\sim 160\ cm^2$  at 20 keV. Passive fine collimators limit the FoV to  $\sim 34'$  square in FWHM. The PIN achieves unprecedented sensitivity in this energy band due to the narrow FoV, the surrounding anti-coincidence detectors, and the low and stable background environment in a low-earth satellite orbit.

The target at (RA, Dec) = ( $12^h 27^m 58^s.9$ ,  $-48^\circ 53' 44''$ ) in the equinox J2000.0 was aimed at the center of the XIS field. The obtained data were processed with the standard pipeline version 2.2, leaving the net exposure time of 30 ks for the XIS and 35 ks for the HXD.

For the XIS, we accumulated source and background signals for the temporal and spectral analyses. The source events were extracted from a  $2'.95$  radius circle around the object encompassing  $\sim 90\%$  of photons, while the background events were from an annulus of  $4'$ – $7'$  in radii. The two XIS FI spectra with nearly identical responses were merged, while the BI spectrum was treated separately.

For the PIN, we simulated background data for the

spectral analysis. The PIN background is composed of instrumental non-X-ray background (NXB) and the cosmic X-ray background (CXB). The NXB spectrum was provided by the instrument team (Fukazawa et al. 2009), while the CXB spectrum was simulated by convolving the HEAO-1 model (Boldt 1987) with the detector responses. We found no contaminating source within the PIN FoV in the INTEGRAL catalogue (Bird et al. 2007).

### 3. Analysis

#### 3.1. Light Curves

We constructed the binned light curves of J12270 (figure 1) after confirming that the background was non-variable. The background-subtracted count rate ( $CR$ ) and the median energy ( $ME$ ) were derived at 0.2–12.0 keV for each bin.  $ME$  is defined as the median of energy of all photons in a bin, serving as a proxy for the spectral hardness suited for low photon statistics (Hong et al. 2004).

The object was occulted by the Earth for  $\sim 1/3$  of each 96 min orbit, causing discontinuities in the light curves. In the following, we call the continuous time spans in the light curves as “intervals”. Variety of temporal features are noticeable at a glance. For example, in  $CR$ , we can see sudden declines (we hereafter call these events “dips”) and rapid amplification (“flares”).  $ME$  is also variable, which shows significant hardening after some flares.

For the quantitative definition of these features, we first

divided the light curves into pieces of a constant  $CR$  or  $ME$  value (“segments”) using a Bayesian blocks (BB) method (Scargle 1998). The algorithm finds the change points of time-variable quantities, at which light curves are better explained by two different constant values before and after the point rather than a constant value. We next derived the base level of  $CR$  and  $ME$  using the third interval (gray shaded region in figure 1), during which no major variability is apparent. The mean and the standard deviation of  $CR$  are 0.67 and 0.22 s<sup>-1</sup>, respectively, while those of  $ME$  are 1.94 and 0.17 keV, respectively. We finally defined dips as segments with  $CR$  below the mean by  $>2\sigma$ , flares as segments with  $CR$  above the mean by  $>2\sigma$ , and “quiescence” for the remaining  $CR$  segments. Similarly, we defined “hard” segments with  $ME$  above the mean by  $>2\sigma$  and “normal” for the remaining  $ME$  segments.

As a result, we found 15 dips (a total of 4.2 ks) with no apparent periodicities and 11 flares (2.5 ks). All the six hard segments (2.5 ks) are preceded by flares. The flares are localized in some intervals, suggesting that the source has X-ray active phases distinctive from quiet phases.

### 3.2. Timing

We employed a generalized Lomb-Scargle algorithm (GLS; Zechmeister & Kürster 2009) for the timing analysis. GLS can process unevenly sampled data and takes the  $CR$  errors fully into account, providing more accurate estimates of the frequency and power than conventional methods. We constructed periodograms up to the Nyquist frequency using selected segments and tested the maximum peak against the local noise. The red noise is dominant, which we derived by phenomenologically fitting with an exponential function (Vaughan 2005). For the flare or dip segments, no significant peak above  $3\sigma$  was found, confirming their lack of periodicity. For all or the quiescent segments, similar negative results were obtained. Figure 2 shows the result for the quiescent segments, in which we found the maximum power at 0.81 mHz, not at the reported RXTE peak. The maximum is slightly above the  $2\sigma$  level, which we regard insignificant.

### 3.3. Spectra

We constructed the background-subtracted spectra in the 0.2–70 keV band using the XIS and the PIN. We produced time-averaged spectrum (figure 3), which is overall featureless including the Fe K complex band (the inset). We also generated spectra for the stacked dip, flare, and hard segments. These spectra are quite similar to the time-averaged one, except for the decreased flux in the soft band for the dip and hard segment spectra.

We fitted the XIS and PIN data simultaneously for the time-averaged and three sets of stacked spectra using a power-law or a thermal bremsstrahlung continuum convolved with an interstellar extinction (*tbabs*; Wilms et al. 2000). All best-fits were acceptable (tables 1 and 2) except for unconstrained bremsstrahlung model for the dip and the hard spectra. Upon the best-fit continuum models, we added a Gaussian model for the tantalizing emission features at 6.5 and 7.0 keV and found that these

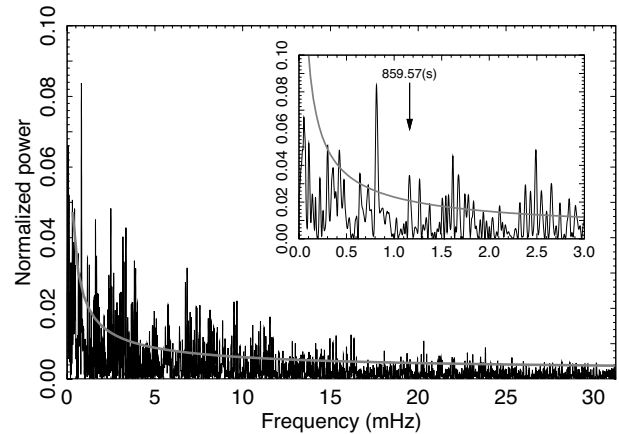


**Fig. 2.** Periodogram of 0.2–12.0 keV data in the quiescent segments. The best-fit red noise profile is shown with the solid curve. The white noise is estimated to be  $\sim 0.002$  in the power. The inset shows a close-up view around the maximum and the previously reported 860 s (Butters et al. 2008) peaks.

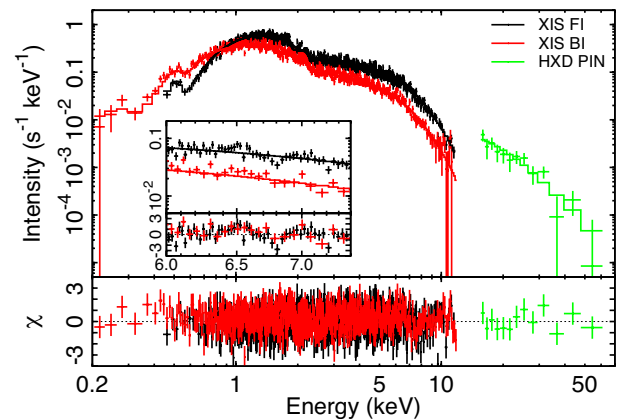


**Fig. 3.** Background-subtracted time-averaged XIS and PIN spectra. The data and the best-fit power-law model are in the upper panel, while the residuals are in the lower panel. The enlarged view in 6.0–7.4 keV is in the inset.

features are insignificant at 90% confidence in the F test.

## 4. Discussion

Our results show that J12270 satisfies none of the defining X-ray characteristics of IPs. First, Fe K $\alpha$  emission is ubiquitously seen not only in magnetic CVs (Ezuka & Ishida 1999; de Martino et al. 2004; Suleimanov et al. 2005) but also in non-magnetic CVs such as dwarf novae (Pandel et al. 2005; Rana et al. 2006). However, we found no evidence of this emission for J12270. The [Fe/H] abundance is  $<0.14$  solar (90%), which is below the typical range (0.2–0.6) for magnetic CVs (Ezuka & Ishida 1999). Second, for the reported 860 s period in Butters et al. (2008), we retrieved their RXTE data and found that the light curve exhibits flares and dips similarly to Suzaku. We confirmed the reported period in the periodogram using all data, but it was rendered insignificant after remov-

**Table 1.** Best-fit parameters for the power-law model\*

State	$N_{\text{H}}$	$\Gamma$	$F_{\text{X}}$	Re- $\chi^2$ (dof)
Average	$1.0^{+0.1}_{-0.1}$	$1.53^{+0.02}_{-0.02}$	$1.82^{+0.02}_{-0.02}$	0.99 (1244)
Dip . . .	$< 0.3$	$1.32^{+0.09}_{-0.07}$	$0.37^{+0.03}_{-0.02}$	1.12 ( 98)
Flare ..	$1.2^{+0.2}_{-0.2}$	$1.62^{+0.04}_{-0.04}$	$4.54^{+0.11}_{-0.11}$	0.90 ( 603)
Hard ...	$2.9^{+1.3}_{-1.3}$	$0.64^{+0.10}_{-0.10}$	$1.70^{+0.27}_{-0.27}$	1.28 ( 141)

\* The parameters are the absorption column density ( $N_{\text{H}}$ ) in the unit of  $10^{21}$  cm $^{-2}$ , the photon index ( $\Gamma$ ), and the 0.2–12.0 keV flux ( $F_{\text{X}}$ ) in  $10^{-11}$  erg s $^{-1}$  cm $^{-2}$ . The ranges of parameter values indicate the 90% statistical uncertainty. The goodness of the fit is indicated with the reduced  $\chi^2$  value (Re- $\chi^2$ ) and the degree of freedom (dof).

**Table 2.** Best-fit parameters for the bremsstrahlung model\*

State	$N_{\text{H}}$	$k_{\text{B}}T$	$F_{\text{X}}$	Re- $\chi^2$ (dof)
Average	$0.6^{+0.1}_{-0.1}$	$16.4^{+1.0}_{-0.9}$	$1.77^{+0.11}_{-0.10}$	1.00 (1244)
Flare ..	$0.6^{+0.1}_{-0.1}$	$11.6^{+1.1}_{-1.0}$	$4.37^{+0.41}_{-0.38}$	0.93 ( 603)

\* The notations follow table 1 except for the electron temperature ( $k_{\text{B}}T$ ) in keV.

ing flares and dips. Third, the occasional flares and the pivots between the quiet and active phases in J12270 is uncommon for IPs except for AE Aqr (Choi et al. 1999). However, the time scales of these behavior in AE Aqr are much longer than J12270. With all the counter-evidence, we conclude that J12270 is not an IP.

The short and aperiodic changes in the X-ray and optical flux suggest that J12270 constitutes an accreting system. The lack of early-type signatures in the unobscured optical spectrum (Masetti et al. 2006) indicates that the secondary is a late-type star. The flux changes in  $\sim 100$  s and the power-law spectrum point toward a LMXB nature of this source. In fact, LMXBs commonly exhibit short bursts and dips. Bursts can be caused by thermonuclear flashes on the neutron star surface (type I) or the sudden increase of the accretion rates due to disk instability (type II). The flares in J12270 are quite similar to those in the Rapid Burster (Lewin et al. 1976), which is the prototypical type II burster, or GRO J1744–28 (Kouveliotou et al. 1996). The flares in these sources commonly show the repetition of short flares, the flux amplification by a factor of  $\sim 5$  from the quiet level, and the flux decrease immediately after some flares.

The distance to J12270 was estimated as  $\sim 220$  pc (Masetti et al. 2006) assuming that the V-band flux is dominated by the secondary. However, the variability with a large amplitude of  $> 1$  mag in this band (Pretorius 2009) indicates that the emission from the accreting material accounts for a substantial fraction. Indeed, a ten-fold increase in the distance estimate can be easily reconciled with observations. If the source is located at 2.2 kpc, the X-ray luminosity is  $\sim 1 \times 10^{34}$  erg s $^{-1}$ , and the height above the Galactic plane is 0.5 kpc, which exceeds the scale height of the Galactic interstellar HI gas (Spitzer 2004). The integrated HI column of  $1 \times 10^{21}$  cm $^{-2}$  in this direction (Kalberla et al. 2005) is consistent with our spectral fitting result (table 1). Both the X-ray luminosity and

the scale height estimated for 2.2 kpc are reasonable for a LMXB (Christian & Swank 1997).

The authors thank J. D. Scargle and M. Zechmeister for providing the BB and GLS scripts, respectively, and K. Mukai, A. Imada and T. Dotani for helpful comments.

## References

- Barlow, E. J., Knigge, C., Bird, A. J., J Dean, A., Clark, D. J., Hill, A. B., Molina, M., & Sguera, V. 2006, MNRAS, 372, 224
- Bird, A. J., et al. 2007, ApJS, 170, 175
- Boldt, E. 1987, Phys. Rep., 146, 215
- Butters, O. W., Norton, A. J., Hakala, P., Mukai, K., & Barlow, E. J. 2008, A&A, 487, 271
- Choi, C.-S., Dotani, T., & Agrawal, P. C. 1999, ApJ, 525, 399
- Christian, D. J., & Swank, J. H. 1997, ApJS, 109, 177
- de Martino, D., Matt, G., Belloni, T., Haberl, F., & Mukai, K. 2004, A&A, 415, 1009
- Downes, R. A., Webbink, R. F., Shara, M. M., Ritter, H., Kolb, U., & Duerbeck, H. W. 2001, PASP, 113, 764
- Ezuka, H., & Ishida, M. 1999, ApJS, 120, 277
- Fukazawa, Y., et al. 2009, PASJ, 61, S17
- Hong, J., Schlegel, E. M., & Grindlay, J. E. 2004, ApJ, 614, 508
- Kalberla, P. M. W., Burton, W. B., Hartmann, D., Arnal, E. M., Bajaja, E., Morras, R., & Pöppel, W. G. L. 2005, A&A, 440, 775
- Kokubun, M., et al. 2007, PASJ, 59, S53
- Kouveliotou, C., van Paradijs, J., Fishman, G. J., Briggs, M. S., Kommers, J., Harmon, B. A., Meegan, C. A., & Lewin, W. H. G. 1996, Nature, 379, 799
- Koyama, K., et al. 2007, PASJ, 59, S23
- Landi, R., Bassani, L., Dean, A. J., Bird, A. J., Focci, M., Bazzano, A., Nousek, J. A., & Osborne, J. P. 2009, MNRAS, 392, 630
- Lewin, W. H. G., et al. 1976, ApJ, 207, L95
- Masetti, N., Palazzi, E., Bassani, L., Malizia, A., & Stephen, J. B. 2004, A&A, 426, L41
- Masetti, N., et al. 2006, A&A, 459, 21
- Mitsuda, K., et al. 2007, PASJ, 59, S1
- Pandel, D., Córdova, F. A., Mason, K. O., & Priedhorsky, W. C. 2005, ApJ, 626, 396
- Patterson, J. 1994, PASP, 106, 209
- Pretorius, M. L. 2009, MNRAS, 395, 386
- Ramsay, G., Wheatley, P. J., Norton, A. J., Hakala, P., & Baskill, D. 2008, MNRAS, 387, 1157
- Rana, V. R., Singh, K. P., Schlegel, E. M., & Barrett, P. E. 2006, ApJ, 642, 1042
- Revnivtsev, M., Sazonov, S., Jahoda, K., & Gilfanov, M. 2004, A&A, 418, 927
- Scargle, J. D. 1998, ApJ, 504, 405
- Serlemitsos, P. J., et al. 2007, PASJ, 59, S9
- Spitzer, L. Jr. 2004, Physical Processes in the Interstellar Medium (Weinheim: WILEY-VCH Verlag), 226
- Suleimanov, V., Revnivtsev, M., & Ritter, H. 2005, A&A, 435, 191
- Takahashi, T., et al. 2007, PASJ, 59, S35
- Vaughan, S. 2005, A&A, 431, 391
- Warner, B. 1995, Cataclysmic variable stars (Cambridge: Cambridge University Press), 1
- Wilms, J., Allen, A., & McCray, R. 2000, ApJ, 542, 914
- Zechmeister, M., & Kürster, M. 2009, A&A, 496, 577